

## Detection and Compensation of the Birefringence

Robert GAROTTA\*, Pierre-Yves GRANGER and Halim DARIU (2005)

### Summary

The effects of birefringence or shear wave splitting on a single raypath recorded with a good signal-to-noise ratio can be easily described and formalized, offering a way of deriving birefringence attributes: natural orientation, percentage of azimuthal anisotropy and differential attenuation. To benefit from a good signal, attributes are most often derived from between the main seismic horizons, limiting the resolution. A brief description of the basic principles and procedures used to define birefringence attributes is presented. A global optimization approach that is able to deliver the birefringence attributes within a 3D block for thinner intervals is proposed.

### Introduction

Birefringence on real data was first observed in well seismic, and then on shear wave lines (Lynn & Thomsen, 1986). It then took some time for our profession to accept that it could also be investigated from PS-converted mode data (Garotta & Marechal, 1987), which is now most commonly used by the industry. Birefringence intervenes at two stages in the seismic process: first, at the imaging stage, birefringence has to be compensated for to avoid a loss in the resolution of the shear or converted mode seismic signal, and then, at the interpretation stage, birefringence attributes are related to lithology. These relationships are of great interest for reservoir characterization.

#### 1) Single-layer birefringence along a raypath

Figure 1 describes the effect of birefringence on a shear propagation generated by a pulse polarized in the radial direction (Fig 1a). In the time domain (Fig 1b), the effect of propagation through the anisotropic layer is the split of the original radial spike into a two-leg operator projected onto the acquisition components, which convolves the seismic wavelet. Each component is defined by the angle ( $\alpha$ ) of the original polarization to the natural orientation S1 and by the delay ( $d$ ) caused by the velocity difference between the S1 and S2 propagations.

Figure 2 defines the size of the S1 or S2 projections along the radial or transverse orientations.

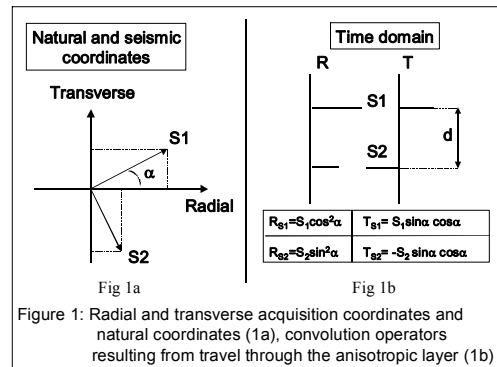


Figure 1: Radial and transverse acquisition coordinates and natural coordinates (1a), convolution operators resulting from travel through the anisotropic layer (1b)

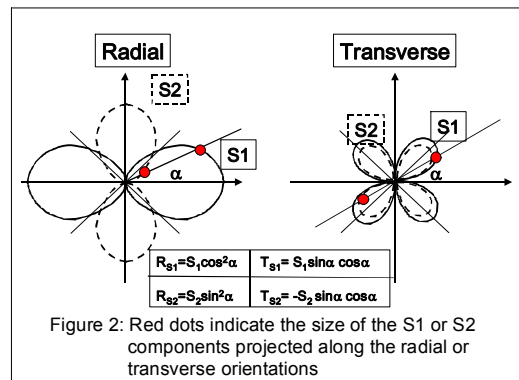


Figure 2: Red dots indicate the size of the S1 or S2 components projected along the radial or transverse orientations

#### 2) Single-layer attribute definition

The basic tool for ( $\alpha$ ) and ( $d$ ) attribute definition is simulation of the rotation of the seismic acquisition coordinates, simply realized by vector projection. The simulation concerns the source and receiver stations in SS mode, and the receiver station only in PS mode. As source polarization does not exist in PS mode, azimuth selection can replace the source rotation in 3D surveys. Two criteria can define the simulated rotation that matches the acquisition and natural coordinates:

- first criterion, the transverse (or cross) component is zero
- second criterion, the simulated components are locally homothetic (should be homothetic after applying the stretch involved by the velocity difference between S1 or S2 propagations)

## Detection and Compensation of the Birefringence

Note that the second criterion works on PS-mode 2D or 3D data, while the first one in PS mode requires 3D data.

The first criterion is used in procedures known as:

- Alford rotation, or pseudo Alford rotation in PS mode (Alford, 1986),
- radial-to-transverse energy ratio (Garotta & Granger, 1988),
- polarity filter,
- and some possible variants.

All these procedures lead globally to equivalent results. Marginal advantages or drawbacks are mainly linked to data handling.

The second criterion (Neville, 1986) retains some optima of the cross-correlation of the S1 and S2 simulated components versus the simulated rotation angle:

- maximum peak value,
- maximum time lag ,
- maximum symmetry, involving more information, is the most robust.

### 3) Multi-layer birefringence

As seen in §1, when the raypath passes through successive anisotropic layers having different natural coordinates, each spike propagating within a layer is replaced by the result of the convolution by the operator characterizing the layer.

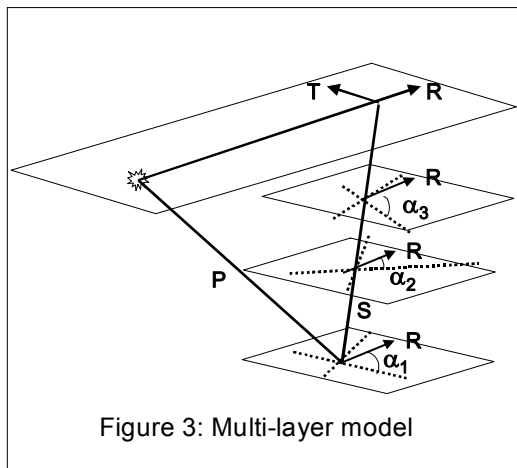


Figure 3: Multi-layer model

In theory, when the original spike travels across  $n$  anisotropic layers it is replaced by a  $2^n$  leg operator. In practice, seismic resolution is reduced.

Figure 3 illustrates an upgoing S-mode path travelling from the conversion point to the surface through layers of

different natural orientations. In order to evaluate their respective attenuations, S1 and S2 components are assumed to have the same amplitude before propagating into the layers.

Figure 4 shows how an original spike is affected in the time domain or in the frequency domain by travelling across sets of three anisotropic layers. Three examples are considered introducing constant time delays between S1 and S2 (5ms) but with increasing natural orientations, respectively by  $15^\circ$ ,  $30^\circ$ ,  $45^\circ$ .

Original spikes are strongly affected, notches appear in the spectra, attenuations may be in the order of 10dB or even higher.

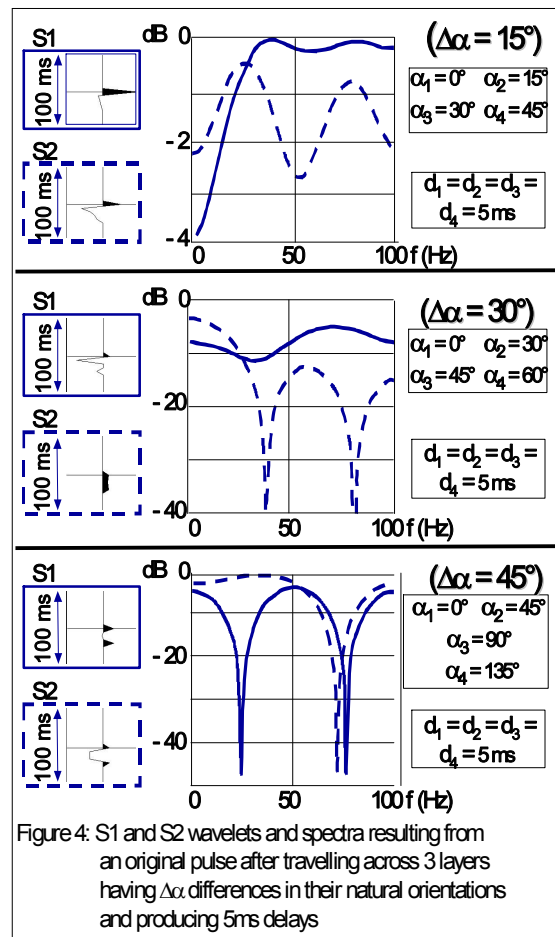


Figure 4: S1 and S2 wavelets and spectra resulting from an original pulse after travelling across 3 layers having  $\Delta\alpha$  differences in their natural orientations and producing 5ms delays

## Detection and Compensation of the Birefringence

### 4) Layer stripping approach

According to the convolution scheme, layer stripping involves defining progressively, from top to bottom, the convolution operators associated with each layer, and compensating for them. This means applying to the data corresponding to the deeper layer an inverse rotation to the one caused by the upper layer and to compensate for the delay induced on the slower component. Layer stripping techniques are generally based on the best seismic horizons and are sequential, with each layer requiring a processing step.

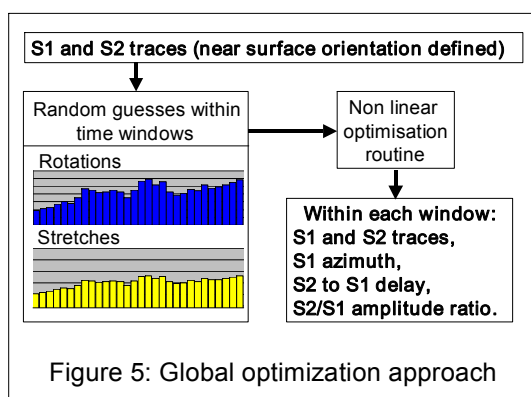


Figure 5: Global optimization approach

### 5) A global optimization approach

In this process, input data consist of two common image stacks polarized respectively along the natural axes of the shallow zone. Time windows of arbitrary length are defined but their length should remain longer than around 1/3 of the dominant period. A global optimization approach (Darius et al, 2005) includes the following steps illustrated in figure 5:

- random guesses of rotations and stretches are applied within each window;
- a given window is submitted to the sum of the rotations and the stretches defined in the upper windows;
- a non-linear optimization routine defines for all time windows the rotations and the stretches which finally reduce to a minimum the differences between the S1 and S2 traces.

The advantages of this procedure are as follows: - an automatic routine does not require intermediate steps; it improves the seismic resolution, it can work on windows shorter than half the dominant period; it provides better attribute definition. Conventional layer stripping, on the other hand, goes from one window to the next; the attribute definition is only based upon the signal contained in the next window whereas, in the global optimization process, any rotation or time delay defined in a given window is applied to the deeper windows, which all contribute to the optimization.

The advantages of this procedure are as follows: - an automatic routine does not require intermediate steps; it improves the seismic resolution, it can work on windows shorter than half the dominant period; it provides better attribute definition. Conventional layer stripping, on the other hand, goes from one window to the next; the attribute definition is only based upon the signal contained in the next window whereas, in the global optimization process, any rotation or time delay defined in a given window is applied to the deeper windows, which all contribute to the optimization.

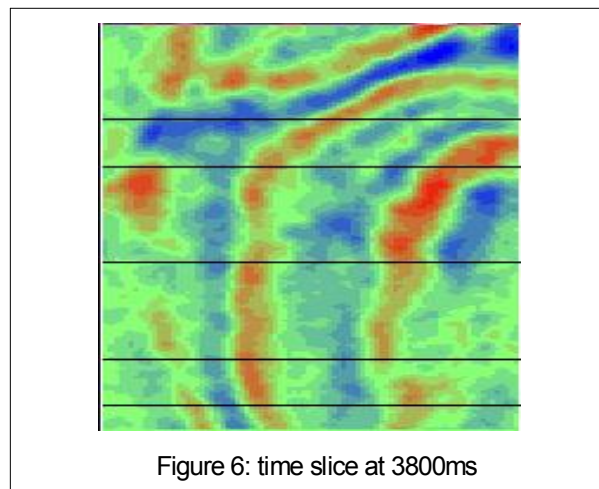


Figure 6: time slice at 3800ms

### 6) Real data example

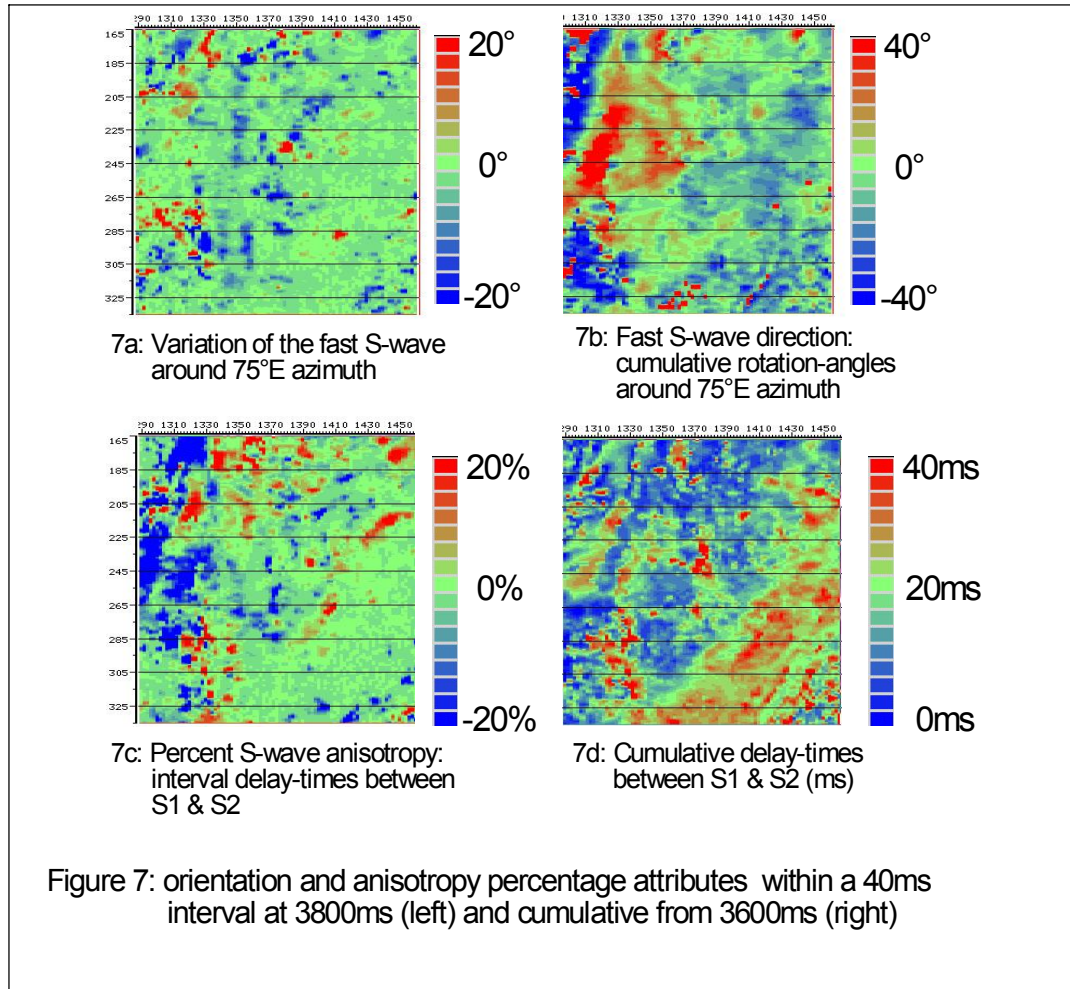
The example (Emilio Field, Adriatic Sea, Italy, courtesy of ENI) shown originates from a pre-processed PS data set where the effects of the shallow to medium depth anisotropy had already been compensated for (Vetri et al, 2003). In figure 6, the time slice at 3800ms is in S1 mode and gives an idea of the structural context. The global optimization process was run within a time gate starting at 3600 up to 4200ms. The time interval retained for deriving local attributes is 40ms PS time, say around 27ms shear time, approximately 40m in depth.

Figure 7 displays the attributes after application of the former compensation. In figures 7a or 7c, rotations or time delays are due to the shear travel time of 27ms only, some isolated red or dark blue spots are probably spurious, but some mainly light blue trends are also indicated. In figures 7b and 7d, representing cumulative effects from 3600ms, organized trends are clearly visible.

### Conclusions

Birefringence effects can be investigated and compensated for in many ways, most of them leading to similar results. A global optimization approach offers advantages regarding the expected accuracy and resolution. The processing turnaround time takes advantage of this automated stripping method.

## Detection and Compensation of the Birefringence



### References

Alford, R.M., 1986, "Shear data in the presence of azimuthal anisotropy," SEG Expanded Abstracts, pp 476-479.

Dariu, H., Granger, P.Y., and Garotta, R.J., 2005, Birefringence analysis using simulated annealing, expanded abstract submitted to 67<sup>th</sup> EAGE conference, this issue.

Garotta, R.J., and Marechal, P., 1987, "Shear wave polarization survey using converted waves," 57<sup>th</sup> Annual International Meeting, SEG, Expanded Abstracts, Session S11-6.

Garotta, R., and Granger, P.Y., 1988, Acquisition and processing of 3Cx3D data using converted waves: 58<sup>th</sup> Annual International Meeting, SEG, Expanded Abstracts, pp 995-997

Naville, C., 1986, Detection of anisotropy using shear wave splitting in VSP surveys: Requirement and Applications, 56<sup>th</sup> Annual International Meeting, SEG expanded abstract, pp 391-394

Lynn, H., and Thomsen, L., 1986, Shear-wave exploration along the principal axes, 56<sup>th</sup> Annual International Meeting, SEG, Expanded Abstracts, pp 473-476

Vetri, L., Loinger, E., Gaiser, J., Grandi, A. and Lynn, H., 2003, 3D/4C Emilio: Azimuth processing and anisotropy analysis in a fractured carbonate reservoir: THE LEADING EDGE, **22**, no. 7, 675-679.